

# Complete Characterization of Polarization-Maintaining Fibers Using Distributed Polarization Analysis

Zhihong Li, X. Steve Yao, *Fellow, OSA*, Xiaojun Chen, Hongxin Chen, Zhuo Meng, and Tiegeng Liu

**Abstract**—We present methods and processes of using a ghost-peak-free distributed polarization crosstalk analyzer (DPXA) to accurately obtain all polarization related parameters of polarization-maintaining (PM) fibers. We show that by first inducing a series equidistant periodic polarization crosstalk peaks along a PM fiber and then measuring the positions and the widths of these peaks using the analyzer, all birefringence related parameters of the PM fiber, including group birefringence, group birefringence variation along the fiber, group birefringence dispersion, and group birefringence temperature coefficient, can be accurately obtained. We further show that the DPXA has the ability to identify and eliminate polarization crosstalk contributions of connectors or splices in the measurement system and therefore can be used to obtain high accuracy measurement of the polarization extinction ratio (PER) of PM fibers. Finally, we propose a set of parameters based on the distributed polarization analysis to quantitatively evaluate the quality of PM fibers. We believe that the methods and processes described in this paper can be widely applied in the industry for the complete characterization of PM optical fibers.

**Index Terms**—Equidistant periodic polarization crosstalk, ghost-peak-free, group birefringence, group birefringence dispersion, polarization-maintaining fiber.

Manuscript received August 9, 2014; revised October 28, 2014; accepted November 25, 2014. Date of publication December 8, 2014; date of current version January 23, 2015. This work was supported in part by the National Basic Research Program of China (973 Program) under Grant 2010CB327806, National Instrumentation Program under Grant 2013YQ03015, International Science and Technology Cooperation Program of China under Grants 2009DFB10080 and 2010DFB13180, China Postdoctoral Science Foundation under Grant 20100470782, the Medical Instruments and New Medicine Program of Suzhou under Grant ZXY2012026, the Foundation Research Project of Jiangsu Province under Grants BK20130373 and BK20130374, and the Internal Development Funding of General Photonics Corporation.

Z. Li and Z. Meng are with the College of Precision Instrument and Opto-electronics Engineering and Key Laboratory of Opto-Electronics Information and Technical Science, Ministry of Education, Tianjin University, Tianjin 300072, China and also with Suzhou Opto-ring Co.Ltd, Suzhou 215123, China (e-mail: zhihong.li2007@163.com; tjictom@126.com).

X. S. Yao is with the College of Precision Instrument and Opto-electronics Engineering and Key Laboratory of Opto-Electronics Information and Technical Science, Ministry of Education, Tianjin University, Tianjin 300072, China and also with General Photonics Corporation, Chino, CA 91719 USA (e-mail: syao@generalphotonics.com).

X. Chen and H. Chen are with General Photonics Corporation, Chino, CA91719 USA (e-mail: jchen1@generalphotonics.com; hongxin.chen@gmail.com).

T. Liu is with the College of Precision Instrument and Opto-Electronics Engineering and Key Laboratory of Opto-Electronics Information and Technical Science, Ministry of Education, Tianjin University, Tianjin 300072, China (e-mail: tgliu@tju.edu.cn).

Color versions of one or more of the figures in this paper are available online at <http://ieeexplore.ieee.org>.

Digital Object Identifier 10.1109/JLT.2014.2377091

## I. INTRODUCTION

**P**OLARIZATION-MAINTAINING optical fiber having a high internal birefringence that exceeds perturbing birefringence for maintaining a linear polarization along the fiber are important to fiber optic communications and fiber optic sensors, particularly fiber optic gyroscopes. The polarization maintaining ability of a PM fiber is generally characterized by polarization extinction ratio (PER) or h-parameter (PER per unit length), while the fundamental parameter governing the performance of a PM fiber is actually characterized by its group birefringence. Therefore, it is important for the manufacturers and the users of a PM fiber to know not only the PER, but also the group birefringence and all other group birefringence related parameters, including group birefringence variations with wavelength (group birefringence dispersion [1], [2]), with temperature (group birefringence thermal coefficient [3], [4]), and along the fiber (group birefringence uniformity [5]).

The PER or h-parameter of a PM fiber can be measured with a polarization cross-talk method specified in standards TIA-544-193 and TIA-544-192 [6], [7], where the 3-dB spectral width of the light source is required to be greater than 10 nm (or the corresponding coherence length should be much less than the differential group delay of the PM fiber under test), for avoiding measurement fluctuations caused by coherent addition of two orthogonal polarization components inside the fiber. However, such a measurement system is cumbersome to set up and the measurement accuracy is susceptible to the birefringence of the lenses and connectors, as well as the misalignment of the polarization inputting to the PM fiber. Commercially available PER meters can be used to directly measure the PER of a PM fiber, however, the measurement accuracy are still limited by 1) the polarization misalignment of light at the input end of the PM fiber under test (FUT), and 2) the polarization misalignments of the light source and its fiber pigtail, and therefore making the measurement of high PER fibers cumbersome and less repeatable.

One or two of the four group birefringence related parameters, as well as PER, can be measured with different implementations of white light interferometer [3], [8]–[11], spectral interferometry [12]–[14], wavelength sweeping technique [15], transient Brillouin grating technique [16], [17], Brillouin optical correlation-domain reflectometry [18], and optical heterodyne detection technique [19]. All those methods are complicated to setup and require in-depth knowledge and extensive know-how to implement. Consequently, their practical use in the industry is limited.

Optical frequency-domain reflectometry for measuring the local birefringence and PER of a short PM fiber taper was reported [20], however, its ability for characterizing a long length of PM fiber with a large number of cross-talk points are yet to be proved.

We reported previously using a distributed polarization crosstalk analyzer (DPXA) to accurately measure the thermal coefficient [4] and dispersion [21] of PM fibers' birefringence. In this paper, we demonstrate methods and processes to simplify the measurements and improve measurement accuracy, and to expand the measurement capabilities of DPXA to include all polarization related parameters, including PER (or h-parameter), group birefringence, group birefringence uniformity, group birefringence dispersion, and group birefringence thermal coefficient. In particular, we introduce a simple fixture to induce a series of polarization crosstalk peaks of equal spacing to assist the measurements. To enable such methods and processes, we devise a mechanism inside the DPXA (General Photonics PXA-1000) to specifically eliminate the ghost interference peaks caused by zero- and 2nd-order interferences of polarization crosstalks [22], and therefore make it possible to obtain the true locations and strengths of a large number of polarization crosstalks along the PM fiber without ambiguity. As will be shown below, the combination of the fixture and ghost-peak elimination simplifies measurement process, reduces many potential measurement errors, and therefore assures accurate measurement results by least trained personnel. Furthermore, we show that the DPXA can readily be used to identify polarization crosstalks induced by the connectors and splices in the measurement setup, and therefore eliminate their contributions to the total PER of a PM FUT, resulting more accurate measurement results without the needs of the careful polarization alignments of light at the input and output ends of the PM FUT. Finally, we propose a set of measurement parameters obtained by a DPXA to quantify the performance of a PM fiber, with test examples of different PM fibers. We believe that the methods and processes described in this paper can be widely applied in the industry for the complete characterization of PM fibers, especially considering that the ghost-peak-free DPXA is becoming commercially available with the efforts of some of the authors [23].

## II. BASIC CONFIGURATION OF DPXA

Fig. 1 illustrates a basic configuration for a DPXA [4], [21]. A polarized super luminescent diode source (SLED) at 1310 nm with a very short coherence length ( $\sim 25 \mu\text{m}$ , corresponding to a 3-dB Gaussian line width of 30 nm) is coupled into the slow axis of a PM FUT (point A of inset in Fig. 1). Assume at point B, a polarization crosstalk is induced by an external disturbance and then some lights are coupled into the fast axis of the PM fiber with a coupling coefficient parameter  $h = I_1/I_2$ , where  $I_1$  and  $I_2$  are the light intensities in the fast and slow axes of the PM fiber, respectively. Because the polarized lights along the fast axis travel faster than that along the slow axis, at output of the fiber the faster light component will be ahead of the slow component by  $\Delta Z = \Delta n Z$ , where  $\Delta Z$  is an optical path

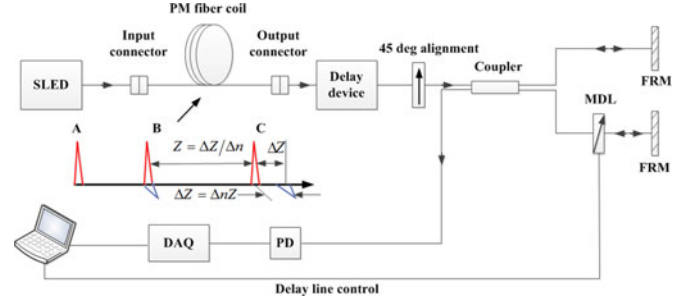


Fig. 1. Illustration of a ghost-peak-free distributed polarization crosstalk analyzer using a scanning white light Michelson interferometer. The inset shows the delay relation between the original and crosstalk components. Light with a short coherence length travelling in the fiber is polarized along its slow axis at input point A. Crosstalk is induced by a stress at point B where a small portion of light is coupled into fiber's fast axis. A relative delay at the output point C between the two polarization components is  $\Delta Z$ . The location  $Z$  of crosstalk point B can be obtained from a measurement of  $\Delta Z$ . FRM, MDL, PD, and DAQ are Faraday rotation mirror, Motor Delay Line, photodetector, and data acquisition card, respectively.

length difference,  $\Delta n$  is a group birefringence of the PM fiber and  $Z$  is the fiber length between the point where the crosstalk occurs (B) and the output end (point C). A polarizer oriented at  $45^\circ$  to the slow axis of the PM FUT was placed at the end of the fiber. Polarization components from both slow and fast axes were projected onto a same direction of the linear polarizer axis so as to produce interference pattern between those two components in a scanning Michelson interferometer. When the relative optical path length is scanned, an interference peak appears when these two polarization components are overlapped in the space but disappears when they are separated more than a coherence length of light source (i.e., SLED). Then the group birefringence  $\Delta n$  of PM FUT between two positions B and C can be calculated as following.

$$\Delta n = \Delta Z / Z. \quad (1)$$

It is evident from eq. (1) that the accuracy of  $\Delta n$  depends on the measurement accuracies of both  $\Delta Z$  and  $Z$ .

Note that the illustration in Fig. 1 assumes only one polarization crosstalk point along the fiber. If there are multiple polarization crosstalk points, second order interference peaks will occur. That is, the light in the fast axis caused from the coupling at a crosstalk point will couple back to the slow axis at the subsequent crosstalk points down the fiber. As shown in Fig. 2(a), consider a situation where there are three coupling points  $X_1$ ,  $X_2$  and  $X_3$  along the PM fiber, and the light input to the PM fiber has no fast axis component and is polarized along the slow axis of the PM fiber. At each coupling point, light is coupled not only from the polarization mode along the slow axis to the polarization mode along the fast axis, but also from the polarization mode along the fast axis to the polarization mode along the slow axis. As a result of this coupling, the resulted wave packet series output by the PM fiber include wave packet caused by multiple couplings. As shown Fig. 2(b), four wave packets include zero order coupling  $S_0$  (no coupling) and the second order couplings  $S_{12}$ ,  $S_{23}$  and  $S_{13}$  emerging at the output

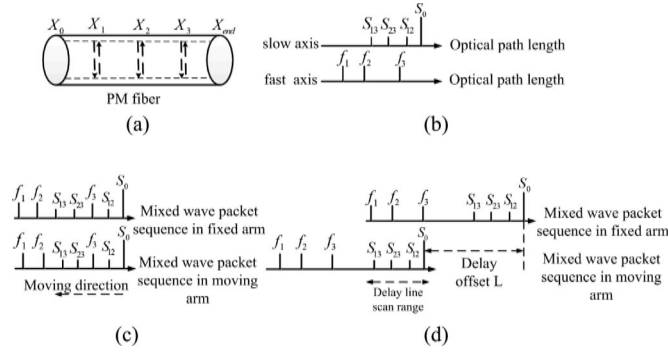


Fig. 2. (a) Illustration of polarization coupling at locations  $X_1$ ,  $X_2$ , and  $X_3$  along the PM fiber, (b) the wave packet sequences polarized along the slow (denoted by S) and fast axes at output of the PM fiber (denoted by f), (c) Wave packets in the two interferometer arms after light passing through the  $45^\circ$  oriented analyzer, where the wave packets aligned to the slow and fast axes are mixed together. When this mixed light is input to the interferometer in Fig. 1, a series of interference peaks, including multiple ghost peaks, will be observed as the delay in one arm of the interferometer is changed; (d) Wave packets in the two interferometer arms after the Delay device in Fig. 1 is inserted between the PM fiber's output and the  $45^\circ$  polarizer's input. This differential delay adds an additional delay between the slow axis and the fast axis of the PM fiber. Only the first order interference peaks between  $S_0$  and  $f_1$  and third order interference peaks between  $f_1$  and  $S_{ij}$  can be generated.

are aligned to the slow axis of the PM fiber and three main packets  $f_1$ ,  $f_2$  and  $f_3$  emerging at the output are aligned to the fast axis of the PM fiber, where they are generated by coupling from the slow axis to the fast axis (the first order coupling) at points  $X_1$ ,  $X_2$  and  $X_3$ , respectively.

After passing through the  $45^\circ$  oriented polarizer, the wave packets aligned to the slow and fast axes were projected onto a same direction of the linear polarizer axis, as shown in Fig. 2(c). When this mixed light is input to the interferometer, a series of interference peaks can be observed as the delay in one arm of the interferometer is changed and these second order couplings will cause ghost crosstalk peaks and result in confusions in simple white light interferometers described in [10], [11], [24]. As shown in Fig. 1, we use a differential group delay (Delay Device) inside a DPXA to remove all the ghost crosstalk peaks from the second order couplings [22], making it possible to accurately identify and measure a large numbers of polarization crosstalks along a PM fiber without ambiguity. In particular, as illustrated in Fig. 2(d), the Delay device adds an additional delay  $L$  between polarization components in the slow and fast axes, and the delay  $L$  in vacuum should be longer than  $\Delta Z$  where the additional delay  $L$  is add to the light polarized along the slow axis of the PM fiber. Thus, the two wave packet sequences from the fast-axis and slow-axis are separated in time (or space) after the light passes through the analyzer. If we preset the same delay offset between the fixed and moving arms in the interferometer and restrict the range of the variable delay line in the moving arm, the undesired zero order ( $S_0$  with  $S_0$ ,  $S_{ij}$  with  $S_{ij}$ , and  $f_i$  with  $f_i$ ) and the second order ( $S_0$  with  $S_{ij}$ , and  $f_i$  with  $f_j$ ) interference signals (ghost interference peaks) will not be generated as the delay line scans. Only the desired first order interference signals ( $S_0$  with  $f_1$ ) and the much weaker third order interference signals ( $f_1$  with  $S_{nm}$ ) will be present. Note that the thirds order peaks are

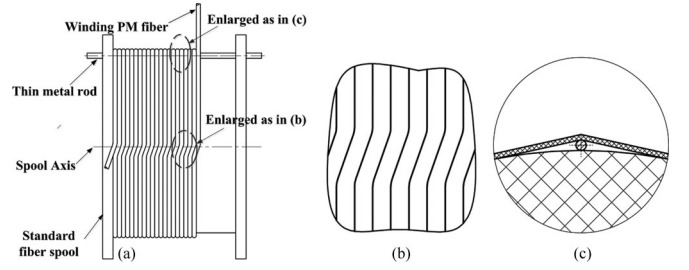


Fig. 3. (a) Illustration of a length of PM fiber wound on a fiber spool with a thin metal rod to induce periodic transversal stresses on the PM fiber at locations the fiber crossing the rod. (b) Detailed view of the fiber when fiber is transitioning from one turn to the next. (c) Detailed view of the fiber when it crosses the metal rod.

negligible (less than  $-75$  dB) if the first order coupling  $f_1$  is less than  $-25$  dB. More detailed description of such ghost-peak-free DPXA can be found in [22].

### III. MEASUREMENT FIXTURE, METHODS AND RESULTS

#### A. Measurement Fixture

To facilitate easy and accurate measurements of group birefringence related parameters, we design a spool-like fixture to induce periodically spaced polarization crosstalk peaks along a PM FUT, as shown in Fig. 3(a). In our experiment, we simply use a standard fiber spool from the fiber manufacturer and affix a piece of thin metal rod with a diameter of 2 mm across its width. A single layer of FUT with a length of 280 m is wound on the spool with a 10-g winding tension and each turn of the fiber is placed closely with the previous turn, as shown in Fig. 3(b). It takes us about four hour for winding such a spool using a simple spool winding machine and the time can be reduced to less than a hour with more practices and process optimization. Re-spooling fiber is a common practice in the industry for fiber manufacturers and fiber spooling/winding machines are commercially available, for example, from Showmark LLC.

As will be shown next, the accuracy of the length of each fiber turn on the spool is critical to the measurement accuracies of the birefringence parameters of the PM fiber to be measured. As shown in Fig. 3, the length  $l$  of each fiber turn is the circumference  $l_c$  of the spool plus the additional length  $\delta_{l1}$  caused by transitioning each turn of fiber to the next (see Fig. 3(b)) and the additional length  $\delta_{l2}$  by the metal rod (see Fig. 3(c)):

$$\begin{aligned}
 l &= l_c + \delta_{l1} + \delta_{l2} \\
 &= \pi d_c + d_c \cdot \left( \sqrt{d_c \cdot d_1} / (d_c - d_1) \right) \\
 &\quad - \arccos \left( (d_c - d_1) / (d_c + d_1) \right) / 2 \\
 &\quad + 2 \cdot d_c \cdot \left( \sqrt{d_c \cdot d_2} / (d_c - d_2) \right) \\
 &\quad - \arccos \left( (d_c - d_2) / (d_c + d_2) \right) / 2. \quad (2)
 \end{aligned}$$

It can be precisely determined when the diameters of the spool  $d_c$ , the fiber  $d_1$ , and the metal rod  $d_2$  are known. In practice, one may use  $l_c$  to approximate  $l$ . For our experiment with  $d_c = 0.17$  m,  $d_1 = 1.65 \times 10^{-4}$  m and  $d_2 = 2 \times 10^{-3}$  m,

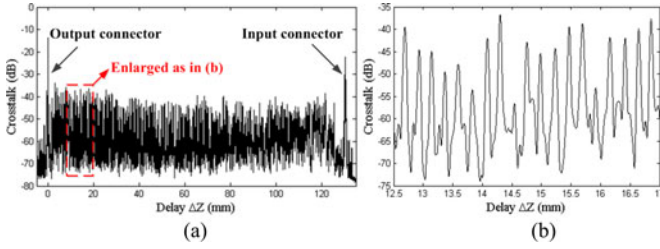


Fig. 4. (a) Polarization crosstalk curve of 280 m PM fiber wound on the spool as a function of the interferometer delay  $\Delta Z$  inside the DPXA. The peaks at the far right and left correspond to the crosstalks induced at the input and output connectors, respectively, from slightly axis misalignment between light polarization and PM fiber axis; (b) the equidistant periodic crosstalk peaks are induced by squeezing of the metal cylinder on the PM fiber.

the relative length error  $(\delta_{l1} + \delta_{l2})/l_c$  for the approximation is about 0.1%. The relative length error can be reduced to less than 0.015% with the metal rod  $d_2 = 5 \times 10^{-4}$  m. Note that the measurement accuracy of the circumference  $l_c$  is about 0.006% when a Vernier caliper is used for measuring the diameter of the spool. In comparison, the fiber length measurement accuracy in [4] is limited by OTDR (optical time domain reflectometer) or a ruler, on the order of 1%.

As expected, “point-like” stresses are automatically applied to the fiber at the points where the fiber goes across the metal rod (see Fig. 3(c)) to produce multiple periodic polarization crosstalks, with a periodicity precisely defined by eq. (2). These periodic crosstalk peaks act like embedded ruler marks on the fiber, which automatically give out precise length information essential for group birefringence related measurements, as required by eq. (1). Note that if the ghost peaks caused by second order coupling are not eliminated, there would be many false peaks between the true periodic peaks, making it difficult to identify the positions of the true peaks.

In practice, such a spool-like fixture can be machined with a precise predetermined diameter (or circumference) and with a thin slot or bump across its width to induce periodic polarization crosstalks, making the embedded ruler more accurate. It is important to point out that the reasons for making such a fixture are 1) to precisely define the lengths between crosstalk peaks, because the accuracy of group birefringence measurement is proportional to the accuracy of such lengths, as shown in Eq. (1), and (2) to create a distribution of crosstalk peaks to reflect the local group birefringences along the fiber. Note that the spatial resolution of the local group birefringence is determined by the circumference of the fixture, on the order of the 0.5 m in our experiment. It can be easily improved by reducing the diameter of the fixture, considering that the spatial resolution of the DPXA is around 6 cm (assuming the group birefringence of the PM fiber is  $5 \times 10^{-4}$ ), although the 0.5 m resolution is sufficient for most PM fiber characterizations.

### B. Group Birefringence and Group Birefringence Uniformity Measurements

Fig. 4(a) is the measured polarization crosstalk curve of a PM PANDA fiber with a diameter of  $6 \mu\text{m}$ , a cladding of  $80 \mu\text{m}$ , and a buffer of  $165 \mu\text{m}$  as a function of the interferometer delay

$\Delta Z$ , showing the polarization crosstalks induced by the line-pressure from the metal rod on the fiber. The peaks at far left and right correspond to polarization crosstalks induced at the output and input connectors respectively due to slightly misalignment of lights coupling into the fiber axis. Fig. 4(b) shows the detailed view of the equidistant periodic crosstalk peaks caused by transversal pressures induced whenever the fiber crosses the metal rod. As one can see that these measured crosstalk amplitudes vary from peak to peak because of the angle variation between the direction of transversal pressure and the fiber’s principal axes during winding the fiber onto the spooling wheel, however such an amplitude variation does not affect the periodicity measurement which is important to the group birefringence measurement. One can readily obtain the spacing between any two stress crosstalk points by simply multiplying the circumference of spool with the number of stress-induced crosstalk peaks between two points. In addition, one can precisely obtain the relative delay  $\Delta Z$  with the encoder of motorized delay line.

When eq. (1) is used to obtain  $\Delta n$ , the total relative error  $\delta_{\Delta n}/\Delta n$  can be expressed as [4]:

$$\begin{aligned} \delta_{\Delta n}/\Delta n &= \sqrt{(\delta_{\Delta Z}/\Delta Z)^2 + (\delta_z/Z)^2} \\ &= \sqrt{(\delta_{\Delta Z}/\Delta n)^2 + (\delta_z)^2}/Z \end{aligned} \quad (3)$$

where  $\delta_{\Delta n}$  is the group birefringence inaccuracy,  $\delta_{\Delta z}$  is the reading error of the delay  $\Delta Z$  of the variable delay line inside the DPXA, and  $\delta_z$  is the measurement error of length  $Z$ . Note that in the previous reports [4], [21], the absolute length of FUT must be accurately measured in order to obtain an accurate group birefringence  $\Delta n$  according to Eq.(3). Any length measurement error will proportionally contribute to the accuracy of  $\Delta n$ . In contrast, here we can use the relative length defined by the circumference of the fiber spool to eliminate the need of absolute length measurement and its associated error, and Eq.(1) can be rewritten as

$$\Delta n = \delta z/(Nl) \quad (4)$$

where  $l$  is fiber length corresponding to the period of the crosstalk peaks defined in Eq. (2),  $N$  is an integer to represent the number of periods we choose in the calculation, and  $\delta z$  is the corresponding delay in the interferometer for the  $N$  periods. The error sources for  $\Delta n$  are from both the relative location inaccuracy  $\delta_{\Delta z}$  between the polarization crosstalk peaks measured with the variable delay line inside the DPXA and the error in the measurement of  $l$ . Note that the delay line generally has an error independent of the traveling distance, we therefore choose to use multiple periodicities ( $N \gg 1$ ) in the experiment to reduce the effect of delay line error  $\delta_{\Delta z}$ , similar to the case of measuring the thickness of a stack of papers in order to accurately determine the thickness of a single paper. We found in our experiment that when  $N \geq 5$ , the measurement uncertainty is sufficiently small. The average  $\Delta n$  obtained is  $\Delta n = 4.65 \times 10^{-4}$  when  $N = 5$ .

Fig. 5(a) shows the variation of  $\Delta n$  as a function of distance  $Z$  along the fiber for the case of  $N = 5$ , where  $Z$  is obtained by dividing  $\Delta Z$  with the average  $\Delta n$  obtained in Fig. 4, as defined in Eq. (1). The large data fluctuations at large distances

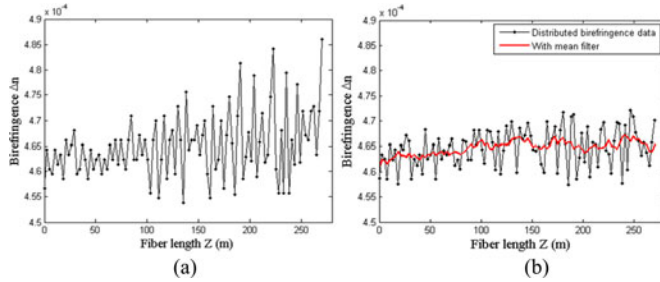


Fig. 5. (a) Measured group birefringence as a function of distance along the 280 m fiber with  $N = 5$  without applying dispersion compensation where the fiber length between any neighboring crosstalk peaks is defined by (2) (0.535 m in the experiment) of the fiber spool. The measurement uncertainty is shown to increase with the distance. (b) The measured group birefringence as in (a), however, the dispersion compensation is applied. The measurement uncertainty at large distances are significantly reduced. The 6-point windowed sweeping average of the group birefringence as a function of distance is shown with the red line. In both (a) and (b), the distance zero is at the position of FUT's output connector.

are caused by the dispersion induced peak broadening due to the group birefringence dispersion [21] to be discussed in Section III-C, because the broadening increase the uncertainty of  $\delta_{\Delta z}$  in Eq. (4). Dispersion compensation procedures described in [21] can be used to further improve the measurement accuracy by multiplying the distributed crosstalk curve with a dispersion compensation function when group birefringence dispersion of the FUT is measured in Section III-C. Fig. 5(b) is the measured group birefringence as a function of distance along the fiber, showing that the measurement uncertainties are greatly reduced when the dispersion compensation procedure in [21] is applied. It is also evident that the mean  $\Delta n$  slightly varies along the fiber length for the FUT.

Note that the tension applied to the fiber when winding the fiber to the spool is not critical to the measurement accuracy. In a separate experiment, we found no noticeable differences in measured birefringence using the same method when three different tension settings (5, 10, and 15 g) of the fiber winding machine were used to wind the spool.

### C. Group Birefringence Dispersion Measurement

As discussed in [21], the envelope of a measured crosstalk peak (i.e., the interference peak) is influenced by SLED's spectral distribution and group birefringence dispersion  $\Delta D$  of the PM fiber. In fact, the envelope width increases quadratically with the distance  $Z$  due to effect of the group birefringence dispersion, and a relationship between envelop broadening  $W$  and group birefringence dispersion  $\Delta D$  can be expressed as [21]:

$$W/W_0 = (1 + (\alpha\Delta D)^2 Z^2)^{1/2} \quad (5)$$

where

$$\alpha = 2\pi c(\Delta\lambda/\lambda_0)^2. \quad (6)$$

In equations above,  $c$  is the speed of light in vacuum,  $\Delta\lambda$  is the 3-dB spectral width of the light source with a Gaussian line shape and  $\lambda_0$  is center wavelength of the light source used for

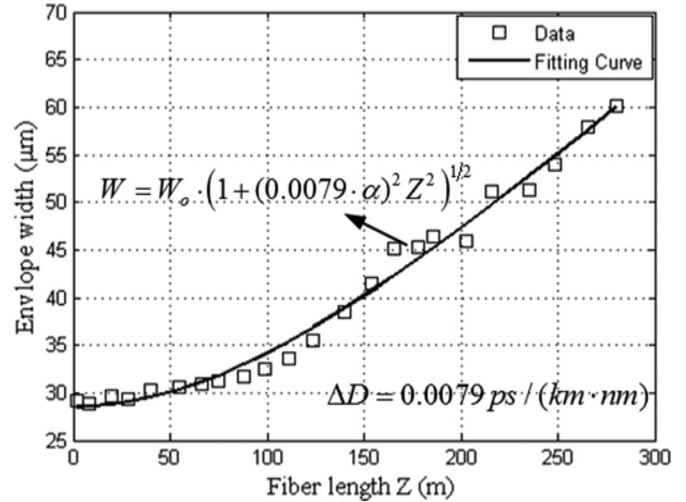


Fig. 6. Envelope widths of crosstalk peaks induced by stress at various locations along the fiber. The envelope widths of polarization cross-talk peaks broaden as fiber length increase due to group birefringence dispersion. Curve-fitting obtains the group birefringence dispersion of the FUT to be  $\Delta D = 0.0079 \text{ ps}/(\text{km} \times \text{nm})$ .

the measurement, respectively, and  $W_0$  is the  $1/e$  width of the interference envelope when the dispersion  $\Delta D$  or  $Z$  equals to zero. As shown in [21], one may simply measure the widths of any two polarization crosstalk peaks with a known spacing  $Z$  between them to obtain the dispersion  $\Delta D$  using (5). However, in order to increase measurement accuracy of  $\Delta D$ , widths of crosstalk envelopes at multiple locations along the PM FUT are measured, and  $\Delta D$  is then obtained by curve-fitting to Eq. (5).

Fig. 6 shows the widths of the crosstalk peaks as a function of their locations along the fiber. The distance is measured from the first induced crosstalk peak and evaluated every 20 peaks ( $N = 20$  or 10.7 m). Unlike in [21] where the locations of crosstalk peaks were calculated using Eq. (1) where the total fiber length  $Z$  must be measured precisely, here only the relative locations are required and they can be precisely obtained by multiplying circumference of the fixture with the peak number, minimizing the error contribution of fiber distance in dispersion measurement. One may argue that the group birefringence dispersion may also be obtained using Eq. (5) by measuring the widths of the crosstalk peaks caused by the output and input connectors, however, the error of the fiber distance measurement also contributes to the dispersion measurement. In addition, such a two-point measurement is sensitive to measurement uncertainties of the widths. The method presented here can effectively avoid such error sources. As can be seen from Fig. 6, the widths of cross-talk peak start to show significant broadening at a distance large than 100 m. The group birefringence dispersion  $\Delta D$  of the PM fiber is accurately obtained by a least-square fitting to Eq. (5) to be  $\Delta D = 0.0079 \text{ ps}/(\text{km} \times \text{nm})$ .

Note that a dispersion compensation function can be obtained once  $\Delta D$  of the fiber is determined, as described in [21]. This dispersion compensation function can be used to remove the broadening of the crosstalk peaks and hence reduce the

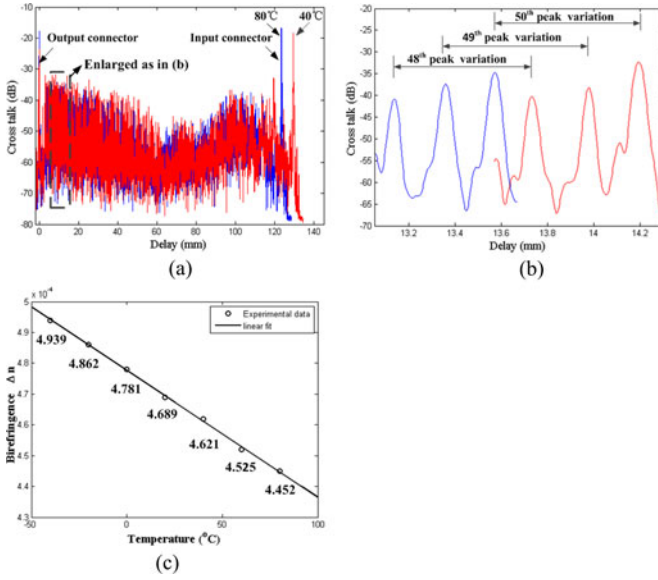


Fig. 7. (a) polarization cross-talk curves of a PM fiber as a function of the relative delay at 80 °C (blue) and 40 °C (red); (b) The expanded view of the positions of the 48st, 49th, and 50th peaks at 80 °C (blue) and 40 °C (red); (c)  $\Delta n$  obtained at seven different temperatures by measuring the spacing between the 1st and the 50th crosstalk peaks at different temperatures using (4).

measurement uncertainties of the group birefringence along the fiber, as described in Section III-B.

#### D. Group Birefringence Thermal Coefficient Measurement

As discussed in [4], the PM fiber is expected to be sensitive to the temperature because of its anisotropic strain that is resulted from differential thermal expansion at different regions in the fiber cladding and is varied linearly with temperature in the vicinity of room temperature. The group birefringence  $\Delta n$  can be written as [4]:

$$\Delta n = \gamma(T_0 - T) \quad (7)$$

where  $T$  is the temperature of FUT,  $T_0$  is the softening temperature of the silica glass with dopants in the stress—inducing region of the cladding, and  $\gamma$  is the thermal coefficient of group birefringence of the PM fiber to be measured.

As in [4], we place the fiber spool of Fig. 3(a) into a temperature chamber, with two fiber pigtailed outside of the chamber. Fig. 7(a) shows two typical polarization crosstalk curves of PM FUT as a function of relative delay for two different temperatures of 80 and 40 °C. Clearly, the positions of all polarization crosstalk peaks are shifted with the temperature, as predicted in Eq. (7). In our previous report [4], we obtain the thermal coefficient of group birefringence by measuring the position of the crosstalk peak induced by the input connector as a function of temperature. However, as described in [4], there are two major error sources affecting the measurement accuracy: 1) fiber length measurement error, and 2) the fiber length outside the temperature chamber. In order to make accurate measurement,

the fiber inside the chamber must be sufficiently long and the fiber pigtailed must be kept sufficiently short.

In this section, we show that both the error sources can be effectively minimized for the following reasons: 1) because the periodic polarization crosstalk peaks induced by the measurement fixture acts as ruler marks along the fiber, the fiber length measurement between any two peaks can be easily obtained with a high precision, and 2) we only measure the relative position variations with temperature between any two periodic crosstalk peaks on the fiber section inside the chamber, and therefore eliminate the error contribution of fiber sections outside of the chamber. In experiment, we choose to measure the spacing  $\Delta Z$  between the 1st and 50th peaks, and measure the group birefringence  $\Delta n$  as a function of temperature. As shown in Fig. 7(b), the peak positions of the 48th, 49th, and 50th peaks shifted to the left as temperature increase, reducing the spacing  $\Delta Z$ . The fact is that the spacing  $\Delta Z$  decreases with the temperature indicates that  $\Delta n$  has a negative thermal coefficient. As mentioned previously a thermal coefficient of the group birefringence  $\gamma$  can be obtained by linear-fitting of  $\Delta n$  to Eq. (7) by using the least square fitting method at each different temperatures. Note that in order to reduce the effect of dispersion, we choose the crosstalk peaks close to the output end of the fiber under test, although dispersion compensation described in Section III-B and III-C may also be used to reduce the peak broadening and improving measurement accuracies for measuring peaks closing to the input connector ( $N \gg 50$ ).

In our experiment we measured  $\Delta n$  for one PM fiber at seven different temperatures (i.e., -40, -20, 0, 20, 40, 60, 80 °C) and the results are plotted in Fig. 7(c). Linear-fitting  $\Delta n$  to Eq. (7) yields a group birefringence thermal coefficient  $\gamma$  of  $-4.123 \times 10^{-7}$ .

#### E. PER Measurement

As mentioned in the introduction, traditional methods described [6], [7] or that using a PER meter for measuring the PER of a PM fiber are susceptible to 1) polarization misalignment at the input end of the FUT, and 2) polarization misalignment between the light source and its fiber pigtail if pigtailed light source is used. Using a DPXA, one can readily identify the crosstalk contributions from the polarization misalignments at the two fiber ends, as well as at the interface between the pigtail and the light source, and eliminate their contributions to the total PER, because the corresponding polarization crosstalk peaks measured with a DPXA are spatially separated. Note that for the PER measurement described in this section, we do not induce the periodic polarization crosstalk peaks as in the previous sections.

Fig. 8 shows the measured polarization crosstalk curves of a PM fiber jumper with FC/PC connectors and a spool of PM fiber of 250 m directly from a PM fiber vendor, fusion spliced with two FC/PC connectors. When a FUT is connected to the DPXA, the polarization misalignment at the connection points induces significant crosstalk peaks. An auto-search program is implemented in the DPXA software to automatically identify

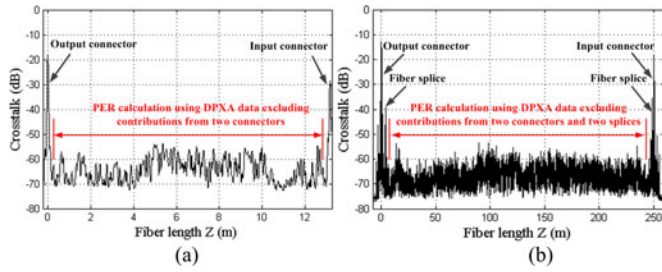


Fig. 8. (a) Polarization crosstalk curves of a 13 m jumper with two FC/PC connectors and (b) a 250 m PM fiber coil spliced with two FC/PC connectors. PER measurement with a commercial PER always including the contributions of the input connector and two splices, while the DPXA has the ability to identify and eliminate polarization crosstalk contributions of all connectors and splices in the measurement system. Note that fiber length in the horizontal axis is obtained by dividing the fiber delay line distance  $\Delta Z$  with the average group birefringence obtained using the procedure described in Section III B.

TABLE I  
COMPARISON OF PER MEASUREMENTS OF A 13 M PM FIBER JUMPER  
AND A 250 M PM FIBER COIL OBTAINED WITH A COMMERCIAL  
PER METER AND A DPXA

Measurement #	PER of Fiber jumper		PER of Fiber coil	
	ERM (dB)	DPXA (dB)	ERM (dB)	DPXA (dB)
1	22.5	34.81	25.7	30.82
2	24.9	34.27	21.8	30.81
3	23.3	35.06	25.4	30.31
4	26.8	34.64	22.5	30.90
5	25.8	35.14	23.8	31.09
Uncertainty (Max-Min) (dB)	4.3	0.87	3.9	0.78

those peaks, because the polarization crosstalk signatures of the fibers inside DPXA are known, as shown in Fig. 8. In addition, the polarization crosstalk peak resulting from the light source and its pigtail is located outside the region defined by the two connectors, and thus is not included for PER calculation. By definition, the PER of the fiber can be calculated as:

$$\text{PER} = 10 \log(P_f/P_s) \quad (8)$$

where  $P_f$  is the total power coupled to the fast axis from the slow axis and can be obtained by integrating of all polarization crosstalks between the two connectors, and  $P_s$  is the total power remain in the slow axis  $P_s = P - P_f$ , where  $P$  is the total received power at the fiber output.

We implement an algorithm in DPXA software to automatically calculate the PER excluding the contributions of the two end connectors from the crosstalk measurement curve, as shown in Fig. 8(a). One may also use the DPXA software to calculate the total PER contribution between any two points along the fiber, and therefore to further exclude the contributions from the two fusion splicing points, as shown in Fig. 8(b). Table I compares multiple PER measurement results of a 13 m fiber jumper and a 250 m PM fiber coil obtained with a commercial PER meter and a DPXA. It is evidence that the PER value obtained by PER meter is several dB smaller than that obtained with a DPXA, due to the contributions of crosstalk from the

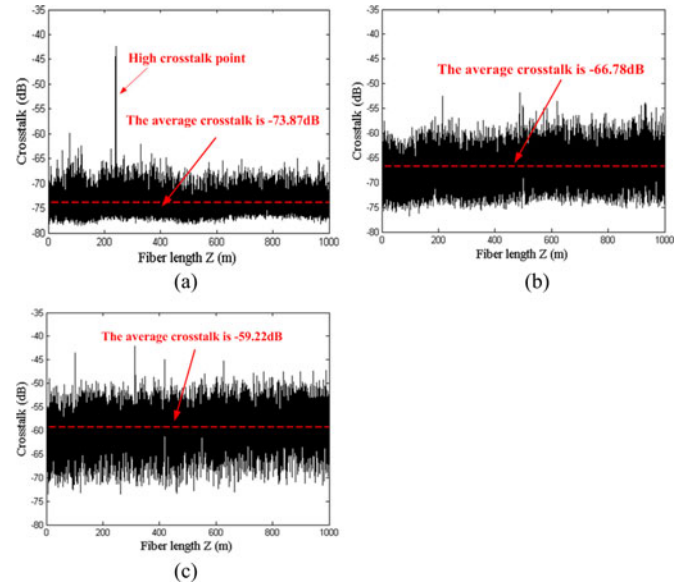


Fig. 9. Polarization cross-talk curves of three different PM fibers. (a) a PANDA PM fiber at 1310 nm with a buffer diameter of 250  $\mu\text{m}$ . A defect point is seen at around 220 m; (b) a PANDA fiber at 1310 nm of the same core/cladding diameters in (a), however, with a reduced buffer diameter of 169  $\mu\text{m}$ ; (c) a third PANDA PM fiber at 1310 nm with the similar cladding diameters as in (a), however, with an even more reduced buffer diameter of 136  $\mu\text{m}$ . Two major defect points with crosstalk more than 45 dB are seen.

polarization misalignment at the input connector. In addition, as anticipated, the measurement repeatability of a DPXA is much better than that of using a PER meter. Therefore, it is much easier to use a DPXA to obtain more accurate PER measurements than using a PER meter.

Note that we used a SLED source with a spectral width around 30 nm when using a PER meter for the PER measurement, in accordance with the requirement of test standard TIA-544-193 [7] to avoid measurement fluctuations caused by coherent effect resulting from the use of a narrow line-width laser [25].

#### F. PM Fiber Quality Evaluation

Up to now, the only parameter that a user can use to characterize the polarization performance of a PM fiber from a vendor is PER or h-parameter, which may not be able to reflect the true polarization performance of the fiber, especially considering that PER measurement using conventional methods may have significant fluctuations as discussed previously. Here we propose to use a set of parameters from a single DPXA scan to fully describe the performance without ambiguity.

Fig. 9 shows DPXA scans of three different PM fibers measured directly with the fiber on the fiber spool from the vendor. We propose to use four parameters to characterize the quality of a PM fiber for the polarization related performance: 1) the average polarization crosstalk, 2) the maximum crosstalk, 3) the number of crosstalk peaks above a certain threshold defined by the manufacturer or the user, and 4) PER. The average crosstalk is the major contributor to the value of PER and closely relates to h-parameter (PER per fiber length). The maximum

TABLE II  
FOUR PARAMETERS TO FULLY CHARACTERIZE THE QUALITY OF THREE DIFFERENT PM FIBERS

	Average crosstalk (dB)	Maximum crosstalk (dB)	Number of crosstalk peaks above -55 (dB)	PER (dB)
Fiber I	-73.87	-42.36	1	28.8
Fiber II	-66.78	-51.88	23	23.6
Fiber III	-59.22	-42.15	1711	16.5

crosstalk is an indication whether the PM fiber is degraded or damaged during manufacturing, packing or shipping of the PM fiber, although a single or few high crosstalk peaks contribute insignificantly to the total PER of a long fiber. For some applications, such as fiber gyro coils, the high crosstalk sections must be removed to assure high quality fiber coil production. A large number of high crosstalk peaks present in the fiber may indicate problems in fiber drawing or packaging process. It also makes it impractical to sort out only good fiber sections for demanding applications.

Table II lists four parameters of the three different fibers under test, obtained from Fig. 9. Fiber I is a commercial PANDA fiber at 1310 nm with a beat length of 2.57 mm, a core diameter of 6  $\mu\text{m}$ , a cladding diameters of 125  $\mu\text{m}$ , and a buffer diameter of 250  $\mu\text{m}$  respectively. Fiber II is a different PANDA fiber at 1310 nm having the same core as Fiber I, but a different beat length of 2.13 mm, a cladding diameters of 80  $\mu\text{m}$ , and buffer diameters of 169  $\mu\text{m}$  respectively. Finally, Fiber III is a third type of PM fiber at 1310 nm with a beating length of 2.6 mm, a core diameter of 6.4  $\mu\text{m}$ , a cladding diameter of 80, and a buffer of 136  $\mu\text{m}$ . It is evident from Fig. 9(a) that Fiber I has the lowest average crosstalk, resulting in a highest PER of 28.78 dB, however, it has a defect point about 220 m from the output connector with a high crosstalk peak of -42.36 dB, probably caused by mishandling when winding the fiber to the spool. Such a defect cannot be identified with a simple PER measurement. We find in experiments that such a defect may be permanent, e.g., cannot be recovered even when the corresponding stress is released. On the other hand, Fiber III has the highest average crosstalk of -59.22 dB, corresponding to a low PER of 16.25 dB. It also has a large number of high crosstalk peaks above -55 dB, probably because the thin buffer layer (136  $\mu\text{m}$ ) cannot effectively protect the fiber from external stresses. Therefore, all four parameters collectively give a full picture of the quality or performance of the PM fiber under test.

#### IV. CONCLUSION

In summary, we demonstrate methods and process of using a ghost-peak-free DPXA to fully characterize all polarization related parameters of a polarization-maintaining fiber, including group birefringence, group birefringence variation along the fiber, group birefringence dispersion, group birefringence temperature coefficient, and PER. In particular, we devise a fixture to induce periodic polarization crosstalk peaks with equal spacing and measure the locations and widths of the peaks to obtain all group birefringence related parameters. The periodicity define by the circumference of the fixture can be used as a build-in ruler to avoid the need for measuring the fiber length, whose measurement error causes a significant error for the group bire-

fringence measurement. In addition, we show that a DPXA is capable to identify crosstalks caused by the polarization misalignments at the fiber input and output ends, as well as at the fiber pigtail of the light source, and to eliminate their contributions to the PER of the fiber, enabling easier and more accurate PER measurements. Finally, we propose a set of parameters from the DPXA measurement of a PM fiber to fully quantify its polarization related performance. We believe that the methods and processes described in this paper can be readily applied in the industry to completely characterize PM fibers with ease and with high repeatability.

#### REFERENCES

- [1] M. Tsubokawa, N. Shibata, T. Higashi, and S. Seikai, "Loss of longitudinal coherence as a result of the birefringence effect," *J. Opt. Soc. Amer.*, vol. A4, pp. 1895-1901, 1987.
- [2] T. Xu, W. Jing, H. Zhang, K. Liu, D. Jia, and Y. Zhang, "Influence of birefringence dispersion on a distributed stress sensor using birefringent optical fiber," *Opt. Fiber Technol.*, vol. 15, pp. 83-89, 2009.
- [3] K. Mochizuki, Y. Namihira, and Y. Ejiri, "Birefringence variation with temperature in elliptically clad single-mode fibers," *Appl. Opt.*, vol. 21, pp. 4223-4228, 1982.
- [4] Z. Ding, Z. Meng, X. S. Yao, X. Chen, T. Liu, and M. Qin, "Accurate method for measuring the thermal coefficient of group birefringence of polarization-maintaining fibers," *Opt. Lett.*, vol. 36, pp. 2173-2175, 2011.
- [5] H. Zhang, G. Wen, Y. Ren, D. Jia, T. Liu, and Y. Zhang, "Measurement of beat length in polarization-maintaining fibers with external forces method," *Opt. Fiber Technol.*, vol. 18, pp. 136-139, 2012.
- [6] *H-Parameter Test Method for Polarization-Maintaining Optical Fiber*, TIA-455-192, 2005.
- [7] *Polarization crosstalk method for polarization-Maintaining Optical Fiber and Components*, TIA-455-193, 2005.
- [8] D. A. Flavin, R. McBride, and J. D. C. Jones, "Dispersion of birefringence and differential group delay in polarization-maintaining fiber," *Opt. Lett.*, vol. 27, pp. 1010-1012, 2002.
- [9] P. L. Francois, M. Monerie, C. Vassallo, Y. Durteste, and F. Alard, "Three ways to implement interfacial techniques: application to measurements of chromatic dispersion, birefringence, and nonlinear susceptibilities," *J. Lightw. Technol.*, vol. 7, no. 3, pp. 500-513, Mar. 1989.
- [10] F. Tang, X. Wang, Y. Zhang, and W. Jing, "Distributed measurement of birefringence dispersion in polarization-maintaining fibers," *Opt. Lett.*, vol. 31, no. 23, pp. 3411-3413, 2006.
- [11] F. Tang, X. Wang, Y. Zhang, and W. Jing, "Characterization of birefringence dispersion in polarization-maintaining fibers by use of white light interferometry," *Appl. Opt.*, vol. 46, no. 19, pp. 4073-4080, 2007.
- [12] M. G. Shlyagin, A. V. Khomenko, and D. Tentori, "Birefringence dispersion measurement in optical fibers by wavelength scanning," *Opt. Lett.*, vol. 20, pp. 869-871, 1995.
- [13] P. Hlubina and T. Martynkien, "Dispersion of group and phase modal birefringence in elliptical-core fiber measured by white-light spectral interferometry," *Opt. Exp.*, vol. 11, pp. 2793-2798, 2003.
- [14] X. Chen, T. Liu, H. Zhang, W. Lu, L. Huang, L. Cheng, and Y. Zhnag, "Spectral-domain measurement of beat length in polarization-maintaining fibers," *Opt. Fiber Technol.*, vol. 18, pp. 527-531, 2012.
- [15] Z.-L. Duan, L.-Y. Ren, Y.-N. Zhang, H.-Y. Wang, B.-L. Yao, and W. Zha, "Theoretical and experimental study of polarization characteristics of polarization maintaining fiber based on wavelength-sweeping modulation," *Microw. Opt. Technol. Lett.*, vol. 52, pp. 1466-1469, 2010.
- [16] Y. Dong, L. Chen, and X. Bao, "Truly distributed birefringence measurement of polarization-maintaining fibers based on Brillouin grating," *Opt. Lett.*, vol. 35, pp. 193-195, 2010.

- [17] Y. Dong, H. Zhang, Z. Lu, L. Chen, and X. Bao, "Long-range and high-spatial-resolution distributed birefringence measurement of a polarization-maintaining fiber based on Brillouin dynamic grating," *J. Lightw. Technol.*, vol. 31, pp. 2981–2986, 2013.
- [18] Y. Mizuno, Z. He, and K. Hotate, "Polarization beat length distribution measurement in single-mode optical fibers with Brillouin optical correlation-domain reflectometry," *Appl. Phys. Exp.*, vol. 2, p. 046502, 2009.
- [19] M. Trubokawa, T. Higashi, and Y. Sasaki, "Measurement of mode couplings and extinction ratios in polarization-maintaining fibers," *J. Lightw. Technol.*, vol. 7, pp. 45–50, Jan. 1989.
- [20] X. Wang, G. Niedermayer, G. Lin, P. Liu, B. Wang, L. Chen, and X. Bao, "Polarization-maintaining property of tapered polarization-maintaining fibers," *Appl. Opt.*, vol. 52, pp. 1550–1554, 2013.
- [21] Z. Li, Z. Meng, X. Chen, T. Liu, and X. Steve Yao, "Method for improving the resolution and accuracy against birefringence dispersion in distributed polarization cross-talk measurements," *Opt. Lett.*, vol. 37, pp. 2775–2777, 2012.
- [22] X. Chen and X. Steve Yao, "Measuring distributed polarization crosstalk in polarization maintaining fiber and optical birefringence material," U.S. Patent number 8, vol. 599, p. 385, 2013.
- [23] (2013). [Online]. Available: [www.Generalphotonics.Com](http://www.Generalphotonics.Com).
- [24] P. Martin, G. Le Boudec, and H.C. Lefevre, "Test apparatus of distributed polarization coupling in fiber gyro coils using white light interferometry," *Proc. SPIE*, vol. 1585, pp. 173–179, 1991.
- [25] A. R. Grant, P. F. Wysocki, and Douglas P. Holcomb, "Polarization effects in polarization-independent and polarization maintaining fiber amplifiers," presented at the IEEE/LEOS Summer Top. Meeting, Quebec City, QC, Canada, 2006.

**Zhihong Li** received the Ph.D. degree in optical engineering from Tianjin University, Tianjin, China, in 2012. From July 2012 to now, he is a Postdoctoral Research Fellow at the College of Precision Instrument and Opto-Electronics Engineering, Tianjin University. His current research interests include optical fiber sensors, including fiber optic gyroscope and the characterization of fiber gyro coils.

**X. Steve Yao (M'97)** received the M.S. and Ph.D. degrees in electrical engineering/electrophysics from the University of Southern California, Los Angeles, CA, USA, in 1989 and 1992, respectively.

He is the Chief Technology Officer of General Photonics Corporation, a California based company that provides the most complete product selections for polarization and timing control for telecommunications and sensor industries. He also holds the National Qianren Scholar Professorship at the Tianjin University in China. He has authored more than 65 referred journal publications, given invited speeches in numerous major photonics-related conferences, and authored a book chapter in RF Photonic Technology in Optical Fiber Links detailing his breakthrough research in optoelectronic oscillator for generating 10 GHz and higher frequency signals. He holds more than 68 issued U.S. Patents and 29 NASA's innovation awards. He worked at NASA's Jet Propulsion Laboratory from 1990 to 2000, concentrating on the research and development of microwave photonic devices and systems, where he invented the optoelectronic oscillator (OEO) for generating the world's cleanest 10–80 GHz signals. He was responsible for the design and demonstration of the X-band fiber optic antenna remoting system for NASA's Deep Space Network. Prior to JPL, he was an Optical Engineer at ADC fiber Optics (a division of ADC Telecommunications) from 1985 to 1987, responsible for developing the first generation of fiber optic wavelength division multiplexing (WDM) devices.

Dr. Yao is a Fellow of OSA, a Topical Editor of Optics Letters, and served as a Member of the Technical Committee in the Optical Fiber Communications conferences in 1998, 2000, and 2001, as the President of the Photonics Society of Chinese Americans in 2011, and as the organization committee member for the Microwave Photonics Conference in 2000. Several products based on his inventions have won multiple industrial awards, including Photonics Circle of Excellence Awards, Laser Focus Innovative Product Awards, and SPIE Prism Awards.

**Xiaojun Chen**, biography not available at the time of publication.

**Hongxin Chen**, biography not available at the time of publication.

**Zhuo Meng**, biography not available at the time of publication.

**Tiegen Liu**, biography not available at the time of publication.